ELSEVIER

Journal of Photochemistry and Photobiology A: Chemistry 149 (2002) 155–168

Journal of Photochemistry and Photobiology A:Chemistry

www.elsevier.com/locate/jphotochem

Photocatalytic degradation mechanism for heterocyclic derivatives of triazolidine and triazole

C. Guillard [a,*], S. Horikoshi [b], N. Watanabe [b], H. Hidaka [b], P. Pichat [a]

[a] *Laboratoire "Photocatalyse, Catalyse et Environnement", CNRS UMR "IFoS", Ecole Centrale de Lyon, BP 163, 69131 Ecully Cedex, France*
[b] *Frontier Research Center for the Global Environment Protection (EPFC), Meisei University, 2-1-1 Hodokubo, Hino-shi, Tokyo 191-8506, Japan*

Received 19 November 2001; accepted 26 November 2001

Abstract

In an attempt to improve the understanding of the basic mechanisms on the degradation of pollutants in water by TiO_2 photocatalysis, we discussed the primary degradation mechanism of three triazolidine derivatives, such as 1,2,4-triazolidine-3,5-dione (TRIANE), 4-hydroxy-1,2,4-triazolidine-3,5-dione (OH-TRIANE) and 4-phenyl-1,2,4-triazolidine-3,5-dione (Ph-TRIANE) and one triazole derivative of the 4-phenyl-1,2,4-triazole-2,5-dione (Ph-TRIOLE), on the basis of the experimental results together with molecular orbital (MO) calculation of frontier electron density and partial charge. The above four heterocycles were selected as molecular probe, principally because the highest frontier electron density was situated at different places of the molecule, while their structures were very similar, two major pathways have been revealed by LC/MS analysis for each heterocyclic compound. The pathway (a) corresponded to the hydroxylation of the atom bearing the highest electron density, via oxidation on nitrogen atom of azo group with respect to the photodegradation of TRIANE, OH-TRIANE and Ph-TRIOLE and opening of aromatic ring when Ph-TRIANE was used. This initial attack occurred with the preferential electrophilic attack of $OH^\bullet$ radicals. The pathway (b) was caused by the attack of active species on to carbon atom of carbonyl group. Considering the calculation of the relative electrophilic density of this carbon atom for the four heterocyclics and the evolution of large amount of N_2 gas at the initial degradation step, it has been suggested that this step (b) was favored by adsorption of carbonyl group on TiO_2 surface as theoretically determined by partial charge and confirmed by IR analysis. The participation of hole (h^+) to form $R–C{=}O^{+\bullet}$ was envisaged in this step. The presence of 1,2,4,5-tetrazixane-3,6-dione also agrees with the participation of TiO_2 surface. The nitrogen inorganic analysis (N_2, $NH_4{}^+$ and $NO_3{}^-$) determined by gas chromatography and ion liquid chromatography, show that the hydrazo group were photoconverted mainly into N_2 gas and partially to $NH_4{}^+$ ions. No nitrate ions were observed at the beginning of the degradation even when a OH substituent was present on one nitrogen atom (case of OH-TRIANE). However, the presence of –OH group increased the $NO_3{}^-/NH_4{}^+$ ratio observed after a few hours of irradiation. The presence of OH also improved the total mineralization of carbon atom into CO_2, which was attributed to mesomeric effect of –OH group. © 2002 Elsevier Science B.V. All rights reserved.

Keywords: Photocatalysis; Titanium dioxide; Photodegradation; Photooxidation; Triazolidine; Triazole

1. Introduction

Heterogeneous photocatalysis over anatase TiO_2, as one of advanced oxidation processes (AOP), is found to be a very efficient method for water and air purification [1–8]. More than 2000 references have been collected on this discipline since about 20 years, 80% of these publications have been written in the last 5 years [9]. A better understanding of the basic mechanisms involved will be useful to improve the efficiency of AOP. However, these mechanisms have been still debated. Can hydroxyl radicals formed on the surface of TiO_2 totally account for the degradation of pollutants or other oxidative pathways also occur [9,10–12]. Every authors of this publication have already contributed to this debate by using different strategies. The intermediate products formed by photocatalysis and by photo-Fenton [13] or used enzyme to scavenge superoxide radicals [14,15] have already been reported. The theoretical determination of radical frontier density to explain the formation of some primary intermediate products by considering $OH^\bullet$ radicals attack was reported [16]. Another important question, which is not often taken into account [17], concerns the role of adsorption on the photooxidative pathway, while it has been shown that efficiency of photocatalysis was linked to electron density and to adsorption on TiO_2 surface [18,19].

One of the aims of this work is to determine the importance of hydroxyl radical attack and of adsorption on the photocatalytic pathway. For that purpose, the following

---

[*] Corresponding author. Tel.: +33-4-72-18-64-94;
fax: +33-4-78-33-03-37.
E-mail address: chantal.guillard@ec-lyon.fr (C. Guillard).

1010-6030/02/$ – see front matter © 2002 Elsevier Science B.V. All rights reserved.
PII: S1010-6030(01)00653-0

strategies were used: (i) choice of several probe pollutants bearing similar structures but the most important frontier density situated at different place of the molecule; (ii) determination of their adsorption by IR data and by theoretical measure of partial charge; (iii) comparison of nitrogen and carbon atom mineralization for the four structures of heterocycles used; (iv) study of the primary intermediate products formed and establishment of pathways; (v) discussion of primary degradation mechanism on the basis of the experimental results together with molecular orbital simulation of frontier electron density. Therefore, this study have chosen three triazolidines with either –H, –OH and/or an aryl ring on the nitrogen atom of the imide and one triazole compound whose structure differs from that of triazolidine in the presence of double bond between both nitrogen atoms.

2. Experimental

2.1. Chemicals and reagents

1,2,4-Triazolidine-3,5-dione (TRIANE), 4-hydroxy-1,2,4-triazolidine-3,5-dione (OH-TRIANE) and 4-phenyl-1,2,4-triazolidine-3,5-dione (Ph-TRIANE) were home prepared while 4-phenyl-1,2,4-triazole-2,5-dione (Ph-TRIOLE) was supplied by Wako Pure Chemicals. The chemical structure is shown below (the atom numbers are used in the molecular orbital calculations):

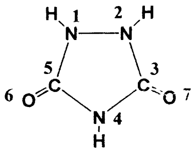

1,2,4-triazolidine-3,5-dione
(TRIANE)

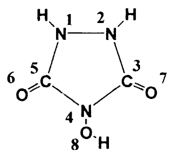

4 - hydroxy-1,2,4-triazolidine-3,5-dione
(OH-TRIANE)

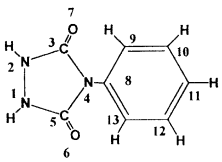

4 - phenyl-1,2,4-triazolidine-3,5-dione
(Ph-TRIANE)

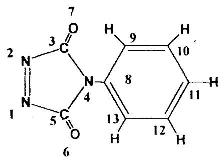

4- phenyl-1,2,4 triazole - 2,5 dione
(Ph-TRIOLE)

Titanium dioxide was Degussa P-25 (particle size, 20–30 nm by TEM image; 80% anatase, 20% rutile by XRD; surface area, 50 $m^2 g^{-1}$ by BET). Deionized and doubly distilled water was used throughout.

2.2. Photodegradation procedures and analytical methods

The magnetically stirred aqueous suspensions were UV-irradiated in a cylindrical pyrex flask (total volume of ca. 124 ml), the reactor was closed. Irradiation was provided by a 75 W mercury lamp having light intensity of ca. 4.0 mW/cm^2 in the wavelength range 310–400 nm (maximum emission, $\lambda = 365$ nm). The sample solution (50 ml, 10^{-3} mol l^{-1}) of initial organic compounds, previously ultrasonicated for 5 min and saturated by oxygen was maintained under magnetically stirred during irradiation in the presence of TiO_2 (2 g l^{-1}) to ensure uniform mixing of the aqueous suspension. The initial aqueous solution after ultrasonication for 5 min previously and saturation by oxygen gas bubbling during 30 min prior to irradiation, 2 ml dispersion after appropriate illumination time was picked up, centrifuged and filtered with Millipore filter (pore size 0.22 μm).

A JASCO V-560 UV/VIS spectrophotometer was used to follow the disappearance of organic compounds in the degraded solution. The formation of ammonium and nitrate ions was determined with a JASCO ion chromatograph equipped with a CD-5 conductivity detector using either a Y-521 cationic column or an I-524 anionic column. A diluted HNO_3 solution (4 mM) and a mixture solution of phthalic acid (2.5 mM)/tris(hydroxymethyl) aminomethane (2.3 mM) were respectively used as an eluent for ammonium or nitrate analysis. The temporal evolution of N_2 and CO_2 gases was monitored by gas chromatography with an Ookura Riken chromatograph (model 802; TCD detector) through a molecular sieve of 5 Å (for N_2 gas) or a Porapack Q (for CO_2 gas) column with helium as the carrier gas. The generation of intermediates in the photodegradation was determined with a Hewlett-Packard LC/MS (electrospray ionization) in the mixed eluent of methanol and H_2O (1:1) equipped with an Agilent Eclipse XDB-column.

2.3. Computer simulations

Computer simulations were performed using the CAChe Worksystem version 3.2 package (Fujitsu) implemented on an Intel P-III and Windows 2000 system. The UV–visible electronic transitions were calculated with ZINDO/1 parameters after geometrical optimization with augmented MM3 and MOPAC PM3. The frontier electron density used to assess the positions of $OH^\bullet$ radical attack and the partial charge in the triazole compounds were also calculated by a MOPAC/PM3 wavefunction.

3. Results and discussion

3.1. Determination of adsorption by theoretical and experimental examination

The initial pH of the four solutions was around 5.5. The surface of the TiO_2 particles is positively charged ($Ti–OH_2{}^+$) at this pH which is below the pzc of TiO_2 Degussa P-25 (≈6.3) [20]. Accordingly, the atoms bearing the greater negative charge of the four compounds could be the preferential points of their adsorption on TiO_2 surface.

Table 1
Partial charge for TRIANE, OH-TRIANE, Ph-TRIANE and Ph-TRIOLE using MOPAC calculation in CAChe package

	TRIANE	OH-TRIANE	Ph-TRIANE	Ph-TRIOLE
N^1	0.065	0.076	−0.053	−0.033
N^2	0.066	0.062	−0.056	−0.032
C^3	0.261	0.297	0.318	0.329
N^4	0.096	0.133	0.117	0.088
C^5	0.261	0.277	0.319	0.328
O^6	−0.632	−0.598	−0.486	−0.362
O^7	−0.632	−0.605	−0.490	−0.362
O^8		−0.271		
C^8			−0.040	−0.030
C^9			−0.150	−0.143
C^{10}			−0.097	−0.094
C^{11}			−0.130	−0.128
C^{12}			−0.099	−0.094
C^{13}			−0.147	−0.143

Partial charges for the nitrogen, carbon and oxygen atoms in the each chemical structure have been simulated by the ZINDO method (see Table 1). As expected, these simulations indicate that the atoms having the most negative charge in the four compounds are the two oxygen atoms while the unsubstantiated nitrogen atoms in Ph-TRIANE and Ph-TRIOLE, and the carbon atoms of the phenyl group bear less negative charge. The nitrogen atoms of TRIANE and OH-TRIANE, and the nitrogen atom linked to aromatic ring bears a positive charge. Therefore, we can estimate that these four compounds adsorb onto the Ti^{VI} surface ions through the carbonyl group.

FT-IR investigations have been performed on TRIANE and OH-TRIANE in the presence or absence of the TiO_2 photocatalyst (see Fig. 1(a) and (b)).

With respect to heterocyclic imides, such as TRIANE, and OH-TRIANE two carbonyl stretches are detected corresponding to in-phase and out-phase stretching of the C=O groups. There are situated at 1792–1778 cm^{-1} and 1694 cm^{-1} for TRIANE molecules and at 1787–1770 and 1673 cm^{-1} for OH-TRIANE molecules. The band at lower wavenumber is always more intense in this type of structure. The in-phase N–H bending corresponds to the IR bands situated between 1444 and 1408 cm^{-1}, but also probably in the shoulder of C=O stretching vibration near 1600 cm^{-1} because its IR spectrum shows the similar pattern to that of a secondary amide when cyclic imide contains a N–H bond [21]. IR bands situated between 1444 and 1408 cm^{-1} were due to the N–H bending of NH–NH structure. The C–N stretching bands were detected at 1332 and 1238 cm^{-1} for TRIANE molecule, and 1341 and 1253–1233 cm^{-1} for OH-TRIANE molecule. The IR band at 1535 cm^{-1} in OH-TRIANE spectrum, not present in TRIANE structure, is probably due to a vibration characteristic band of NOH group. The modification of the stretching vibration of C=O band at 1694 cm^{-1} or at 1673 cm^{-1}, respectively, for TRIANE and OH-TRIANE, i.e. relative decrease of the intensity

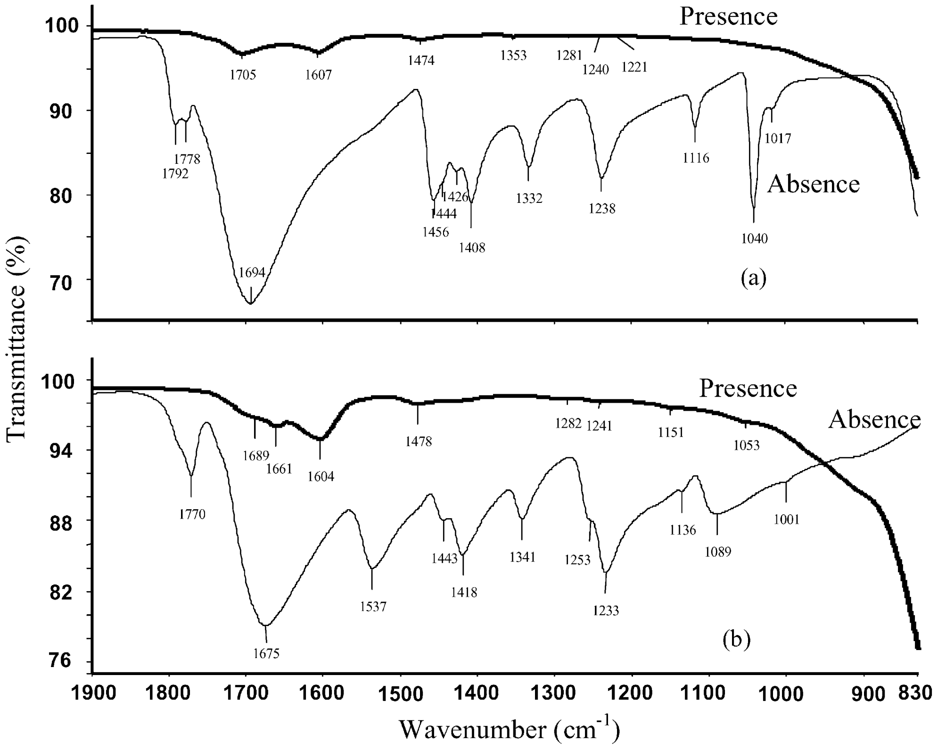

Fig. 1. FT-IR spectra of (a) TRIANE and (b) OH-TRIANE in the presence and absence of TiO_2 photocatalyst.

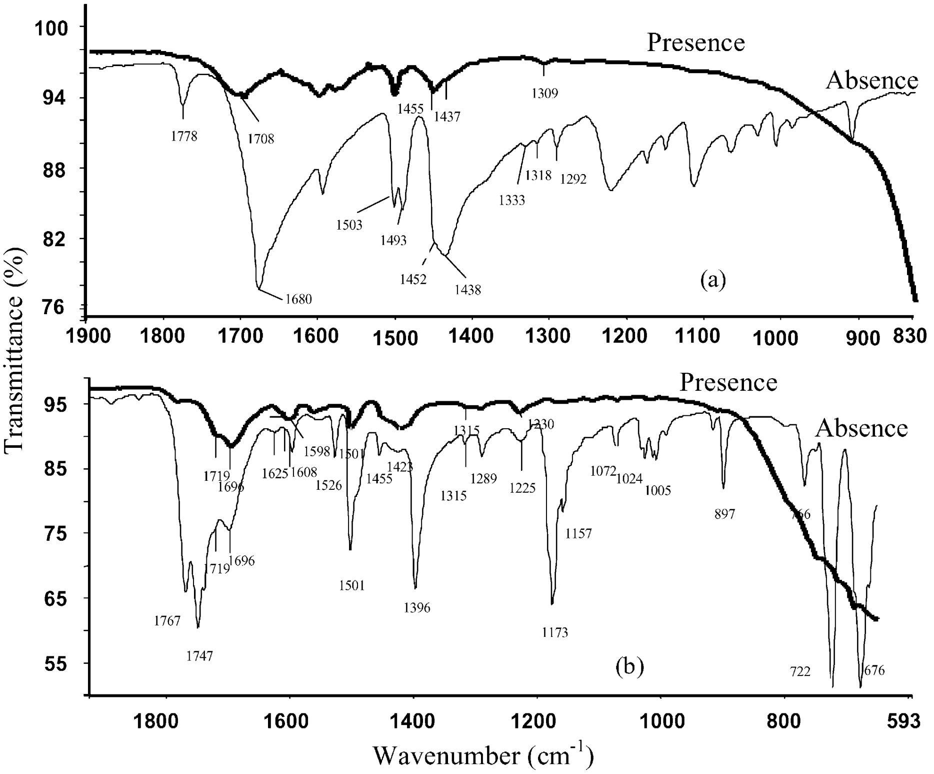

Fig. 2. FT-IR spectra of (a) Ph-TRIANE and (b) Ph-TRIOLE in the presence and absence of TiO_2 photocatalyst.

of IR band, caused by the presence of TiO_2 indicates that the adsorption involved carbonyl group. This experimental result agrees with adsorption envisaged by considering the partial charge determined theoretically. Both molecules may be adsorbed perpendicularly to the surface of titania or obliquely. However, in the case of TRIANE, it is difficult to determine if NH of imide or NH–NH involved in the adsorption. With respect to OH-TRIANE, the disappearance of 1537 cm^{-1} IR band, characteristic of the NOH group, while N–H bending of NH–NH and C–N stretching were always present, seems to indicate that OH-TRIANE is adsorbed by C=O and OH groups of the molecules. This behavior is consistent with the partial charge determined theoretically.

FT-IR spectrums of Ph-TRIANE and Ph-TRIOLE performed in the presence and absence of the TiO_2 photocatalyst are presented in Fig. 2(a) and (b).

Both the stretching vibration of C=O band and the N–H bending situated, respectively, at 1680 and 1452–1438 cm^{-1}, relatively decrease in intensity. The C–N stretching at 1223 cm^{-1} also totally disappeared while both the characteristic band of aromatic ring at 1595, 1503–1493 cm^{-1} and the C–N stretching between imide cycle and aromatic ring were always present. All these observations indicate that the adsorption occurs mainly between TiO_2 surface and CO–NH part of heterocycle and not with aromatic ring. Similar behavior occurred for Ph-TRIOLE. The stretching vibration of C=O band and the C–N stretching of amide and imide, situated, respectively, between 1696–1767, 1396 and 1173 cm^{-1} relatively decreased in intensity or disappeared, while the characteristic band of the aromatic ring at 1501 cm^{-1} and near 1600 cm^{-1} were not modified.

3.2. Photocatalytic degradation

UV absorption spectral features of TRIANE and OH-TRIANE at various irradiation times are illustrated in Fig. 3(a) and (b).

Results of simulated calculations of the initial UV absorption spectrum of TRIANE by the calculation of ZINDO suggested that the absorption between 190 and 206 nm in the spectrum of 0 h in Fig. 3(a) was composed of three UV spectral bands. The absorption at 206 nm was due to UV absorption by O=C–NH–NH–C=O moiety, while C=O groups were the major contributors for the absorption at 200 nm. The O=C–NH–C=O moiety mainly absorbed at 190 nm. The evolution of UV spectrum during the irradiation shows a UV absorption in the 190–206 nm range decreased in intensity and a slight blue-shift occurred at 194 nm. According to simulated calculations of UV spectrum, in a first time probably a breaking of O=C–NH–NH–C=O occurred while O=C–NH–C=O structure persisted a longer time. However, after a long time (7 h) an absorption band at 200 nm appeared. This UV band could be due to the formation of coupling reaction. The UV absorption of OH-TRIANE, Fig. 3(b) displayed one band in the 193–206 nm range. Results of the

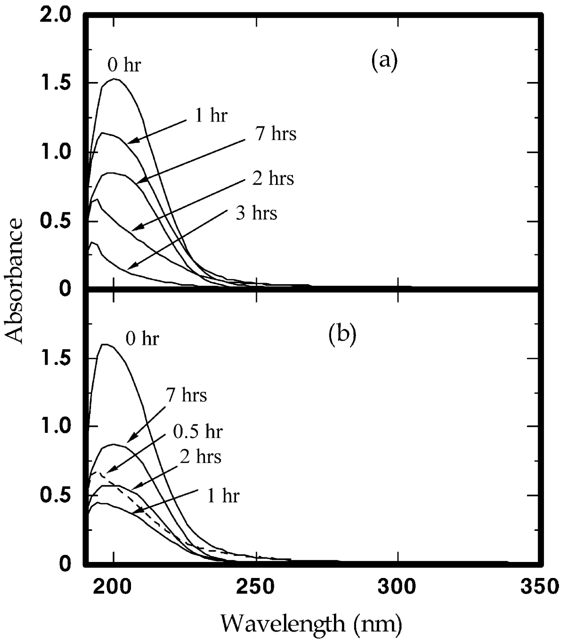

Fig. 3. Temporal UV spectral changes during the photocatalytic degradation of (a) TRIANE and (b) OH-TRIANE.

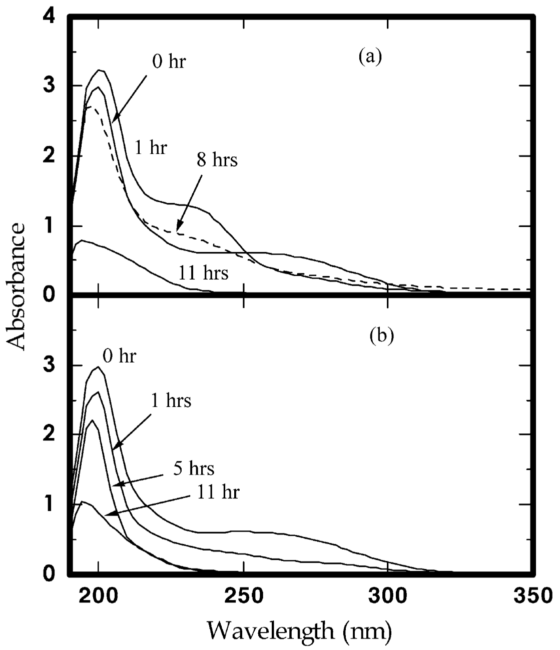

Fig. 4. Temporal UV spectral changes during the photocatalytic degradation of (a) Ph-TRIANE and (b) Ph-TRIOLE.

theoretical simulations suggested that this absorption was due to UV absorption by the O=C–NH–NH–C=O fragment. The UV absorption of O=C–N(OH)–C=O would be situated at 308 nm. This absorption band was not detectable under the conditions.

The evolution of UV spectrum of OH-TRIANE after irradiation indicates that until 1 h of irradiation a decrease of this absorption occurred with a moving near the shortest wavelength. However, like in the case of TRIANE, an increase of the band at 200 nm occurred. This increase appeared earlier than in the case of TRIANE. As previously mentioned, the formation of a condensation product could be at the origin of the new UV absorption band. UV absorption spectral features of Ph-TRIANE and Ph-TRIOLE at various irradiation times are illustrated in Fig. 4(a) and (b).

The UV absorption spectrum of Ph-TRIANE displayed two bands at 252 nm and in the 192–205 nm range (see Fig. 4(a)). After 1 h of irradiation of Ph-TRIANE/TiO_2 dispersion, important modification of UV spectrum occurred. Two new bands appeared at 239 and 285 nm, while a blue-shift of the absorption in the 192–205 nm occurred. ZINDO simulation of the band in the 192–205 nm range showed that the electronic transition implicated states whose wave functions are formed mostly from O=C–N absorption in 192–197 nm without phenyl conjugation, O=C–N–N–C=O absorption at 197 nm and C=C in aromatic ring at 203 nm. The UV absorption in 241–248 nm range was due to the absorption of C=O band. According to this simulation, the transformation of UV spectrum was probably due to the modification of the electronic transition implicated in C=C bond of aromatic ring and in O=C–NH–NH–C=O band by modification of the conjugation. The solution colored into yellow-brown. When the color has totally disappeared, i.e. after about an irradiation of 11 h, only one UV absorption band at 194 nm persisted due to the O=C–N group.

The UV absorption of Ph-TRIOLE (see Fig. 4(b)) consisted of two major bands, one in the range 195–206 nm and the other at 263 nm, as well as a shoulder at ca. 225 nm. Both bands decreased in intensity with increasing irradiation time with the 263 nm band and the shoulder at 225 nm completely disappeared after 1 h. The band at longer wavelength probably due to O=C–N=N–C=O indicated that the initial degradation begin on the heterocycle and not on the aromatic ring.

The temporal evolutions of CO_2 produced in the course of the photodegradation of TRIANE, OH-TRIANE, Ph-TRIANE and Ph-TRIOLE are illustrated in Fig. 5.

The carbon atoms of 70% in TRIANE were mineralized by UV illumination of 5 h. In presence of an aromatic ring on N^4 of triazolidine cycle, it was 92%. In the three cases, the carbon atoms in the molecule for 0.6–0.7% are not mineralized, so the presence of hydroxy or aromatic ring did not influence the number of carbon which were not mineralized. However, when a N=N double bond was present, a total mineralization occurred.

The presence of –OH group in place of H atom on the N^4 atom completely modified the rate of carbon dioxide evolved. The rate of CO_2 appearance for TRIANE and OH-TRIANE were, respectively, 0.4 and 1 μmol/min, i.e. a mineralization rate about 2.5 times higher when OH was present. This result is in accord with the attack by

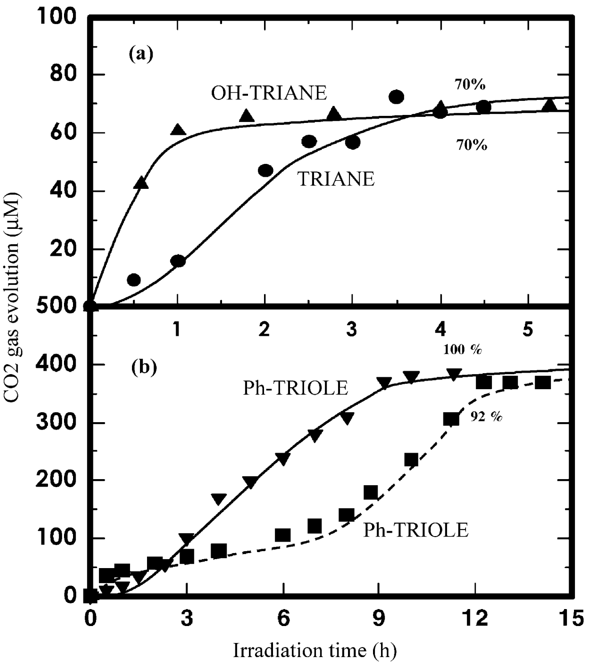

Fig. 5. Evolution of CO_2 in the photooxidation of (a) TRIANE, OH-TRIANE and (b) Ph-TRIANE and Ph-TRIOLE.

electrophilic species since –OH group can activate the reaction due to its electron donor effect.

When an aromatic ring is present on the TRIANE cycle, in a first time, one carbon evolved into CO_2 at the beginning of the degradation, however, after only 0.5 h the mineralization stopped. At the same time an important yellow-brown color appeared which begin to disappear after about 8 h. This irradiation time corresponded to the increase of the release of CO_2. The presence of triazole cycle instead of triazolidine structure modified the degradation pathways. At the beginning, evolution of CO_2 was not found but appeared after 2 h of irradiation.

The temporal formation of nitrogen ions (NO_3^-, NH_4^+) and evolution of N_2 gas produced in the course of the photodegradation of TRIANE, OH-TRIANE, Ph-TRIANE and Ph-TRIOLE are illustrated in Figs. 6 and 7.

In all cases, N_2 gas was formed from the beginning of the degradation. In the case of TRIANE, OH-TRIANE and Ph-TRIANE, about the same percentage 17% of the expected value if all nitrogen atoms were transformed into N_2 gas while in the case of Ph-TRIOLE degradation a more important amount of N_2 gas occurred, about 27% of the expected value. However, the presence of –OH moiety on nitrogen atom and the presence of a N=N double bond between the both nitrogen increased the rate of N_2 gas evolution. As expected [22,23], NH_4^+ ions appeared before NO_3^- ions even in the case of OH-TRIANE where one of nitrogen atom was already oxidized. The oxidation degree of nitrogen atom in OC–NR–CO is −1 when R = OH while it is −3 when R = H as in NH_4^+. Formation of NO_3^- ions exhibited an induction period, showing that several steps of nitrogen oxidation had to occur before evolve under nitrate ions. The formation of NO_3^- ions can come from organic nitrogen atom or from NH_4^+ ions. It is well known that NH_4^+ ions is slowly transformed into NO_3^- by photocatalysis [24]. The presence of nitroso, nitro and *N*-hydroxy organic compounds (Schemes 1, 2 and 5) showed that NO_3^- ions can come from the oxidation of organic nitrogen. The presence of hy-

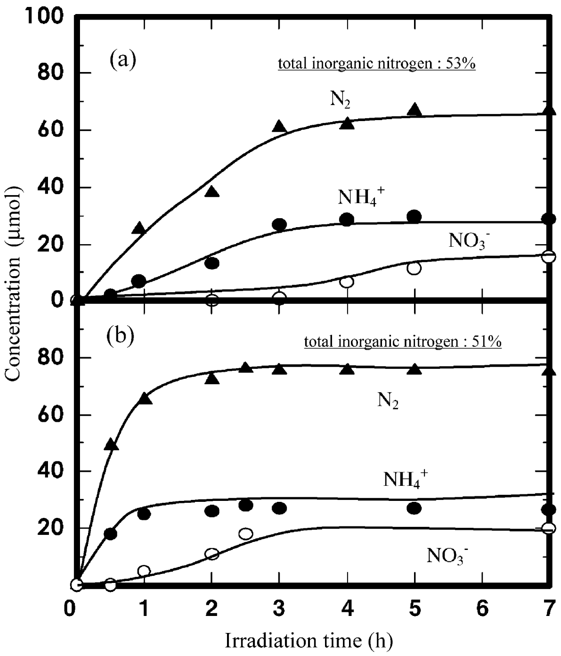

Fig. 6. Formation of NH_4^+, NO_3^- ions and N_2 gas in the photooxidation of (a) TRIANE and (b) OH-TRIANE.

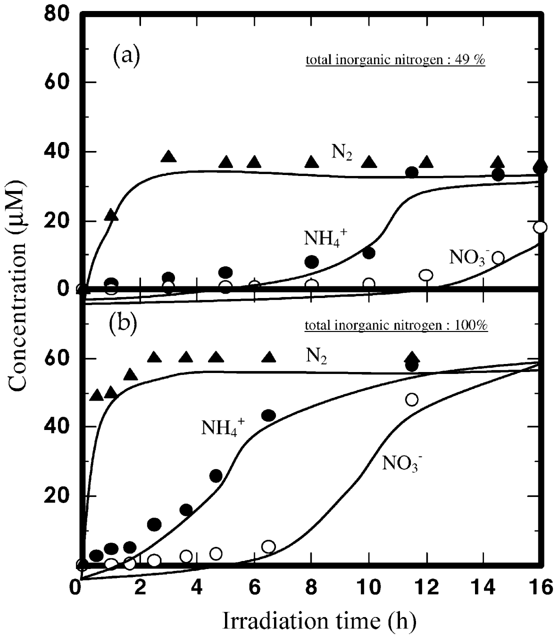

Fig. 7. Formation of NH_4^+, NO_3^- ions and N_2 gas in the photooxidation of (a) Ph-TRIANE and (b) Ph-TRIOLE.

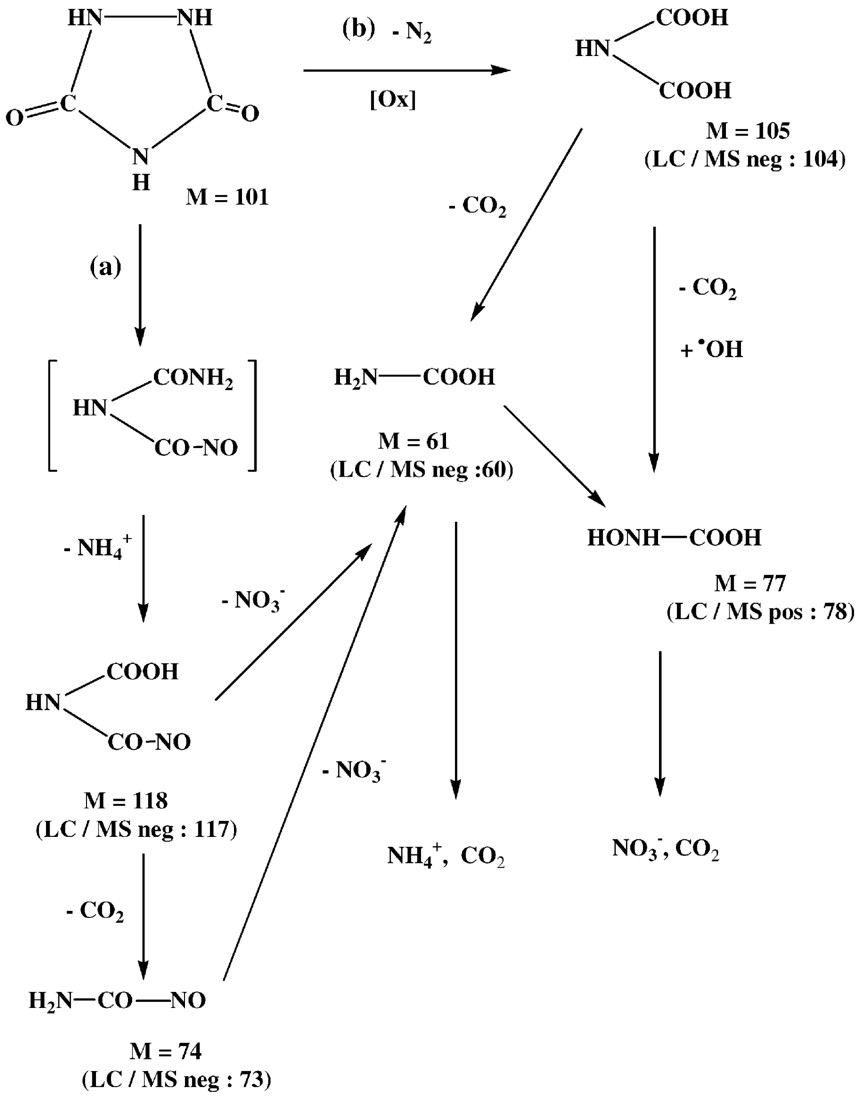

Scheme 1. Proposed pathway for the photodegradation of TRIANE.

droxyl group on nitrogen atom improved the rate of NH_4^+ and NO_3^- ions as previously observed on the rate of mineralisation into CO_2 and N_2 gases. However, it is interesting to notice that the amount of N_2 gas and NH_4^+ ions were equivalent, in the degradation of TRIANE and OH-TRIANE at same CO_2 gas conversion. For example, after about 60% of conversion onto CO_2 gas, i.e. 3 h in TRIANE degradation and 1 h in OH-TRIANE degradation, the amount of N_2 gas and NH_4^+ ions were, respectively, 60 and 25 μmol in both reactions. However, the concentration of NO_3^- ions formed in the case of OH-TRIANE degradation was higher than those detected in the three other degradations at same CO_2 gas conversion, when a steady state was reached. This phenomenon was presumably due to a higher concentration of NO_3^- ions coming from organic nitrogen. In the degradation of Ph-TRIANE, NH_4^+ ions slowly appeared until about 10 h, time corresponding to the decoloration of the solution and then rapidly increased.

This behavior could be attributed to a screening effect of intermediate products. The overall conversion yield of nitrogen atom were around 50% for the degradation of TRIANE, OH-TRIANE and Ph-TRIANE while it was around 90% in the degradation of Ph-TRIOLE.

3.3. Identification of intermediate products by electrospray mass spectroscopy

Identification of intermediate products was derived from LC/MS spectrometric techniques by using both positive {[species + H]:(M + H) or [species + Na]:(M + Na)} and negative {[species − H]:(M − H)} ions.

TRIANE. After about 1 h of irradiation some peaks appeared simultaneously at 88, 104 and 117 *m*/*z* (M − H) which can be assigned to the chemical structures CHO–NH–COOH, COOH–NH–COOH and COOH–NH–CO–NO, respectively. At the same time a signal at 62 *m*/*z* (M − H)

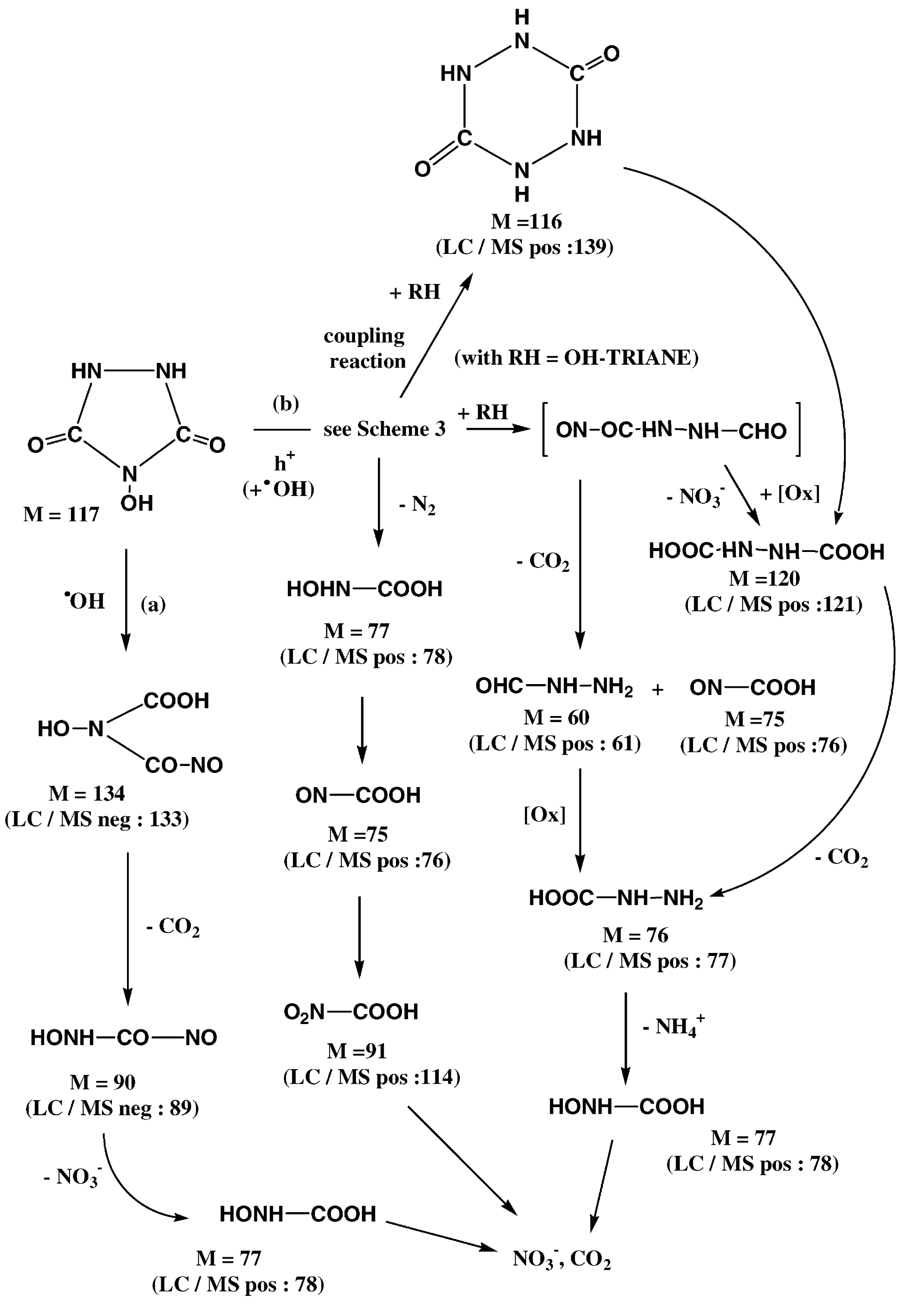

Scheme 2. Proposed pathway for the photodegradation of OH-TRIANE.

assigned at the chemical structure HOCH$_2$–NHOH was observed pointing out the presence of reduction reaction. Two important signals at 73 *m/z* (M − H) and 78 *m/z* (M + H) were detected at 2 h of irradiation, which correspond to the structures NH$_2$–CO–NO and HONH–COOH, respectively. At this irradiation time the structure NH$_2$–COOH just begin to appear in negative mode (60 *m/z*).

OH-TRIANE. From the beginning of the degradation a huge number of intermediates appeared, peaks at 61, 76 and 77 *m/z* (M + H) corresponding to the chemical structures of CHO–NH–NH$_2$, NO–COOH and HOOC–NH–NH$_2$. In negative mode, two other compounds were also detected with M − H equal to 133 and 89 *m/z*. We assigned them to the chemical structures of HOOC–NOH–CO–NO and HOHN–CO–NO. After 1 h of irradiation, all this compounds were always present, and another peak at 114 *m/z* (M + Na), due to the formation of NO$_2$–COOH, appeared. After 2 h, the chemical structures HOHN–CO–NO and CHO–NH–NH_2 still remained and three other signals rose at 78 *m/z* (M + H), 138 *m/z* (M + Na) and 121 *m/z* (M + H). These chemical structures are assigned to HOHN–COOH, $C_2H_4N_4O_2$ (1,2,4,5-tetrazixane-3,6-dione) and HOOC–NH–NH–COOH. As previously observed in the degradation of, H-TRIANE, a signal at 62 *m/z* (M − H) was also detected from the beginning of the degradation, which was attributed to HONH–CH_2OH and correspond to a reduction reaction.

Ph-TRIANE. After 15 min of UV illumination, Ph-TRIANE signature totally disappeared, two new peaks rose in positive mode (M + Na) at 190 and 174 *m/z*. These are attributed to the opening of triazolidine cycle, removing of one carbonyl group and hydroxylation or not of aromatic ring to form 4-phenylsemicarbazide and 4-hydroxyphenylsemicarbazide, respectively. The former intermediates totally disappeared between 3 and 4 h. After 3 h, a signal at 222 *m/z* (M + Na), corresponding to the presence of three hydroxylation of the cycle, appeared, suggesting gradually the hydroxylation of aromatic ring. After 1 h, two new signals appeared in positive mode at 144 and 122 *m/z* which are attributed to (M + Na) and (M + H) of the *N*-phenyl formamide structure. It increased until 5 h of irradiation and then decreased. A signal at 160 *m/z* (M + Na) appeared from 4 h of irradiation showing the oxidation of aldehyde group. An important new signal rose from 6 h of irradiation at 78 *m/z* (M + H) which can be attributed to HONH–COOH as previously detected in the degradation of TRIANE and OH-TRIANE. The MS spectral pattern seen after 11 h of irradiation displayed a signal at 61 *m/z* (M + H), which was the signature of H_2N–NH–COH produced after degradation of aromatic ring.

Ph-TRIOLE. The photodegradation of Ph-TRIOLE during the initial stage yielded peaks at 182 *m/z* (M + H) and 232 *m/z* (M + Na) corresponding to C_6H_5–N$(COOH)_2$ and (C_6H_5)–N(COOH)(CO–N=NOH), respectively. Both signals disappeared after 1 h. The presence of two new peaks at 100 min of irradiation, having values 122 and 138 *m/z* (M + H) in positive mode and attributed to C_6H_5–NH–CHO and C_6H_5–NH–COOH, pointed out the degradation of aliphatic chain. Irradiation for 1 h led also to the breakdown between aromatic ring and triazole cycle to form benzoquinone and 1,2,4-triazole-2,5-dione, both detected in negative mode of 107 and 98 *m/z* (M − H). From 100 min of irradiation, an important signal at 78 *m/z* (M + H) rose until 6.5 h was assigned at HOOC–NHOH coming from *N*-carboxyaniline and dicarboxylic amine. Peaks at 248 and 264 *m/z* in positive mode appearing at 2.5 h of irradiation were assigned to hydroxylation of aromatic ring of the structure C_6H_5–N(COOH)(CO–N=NOH).

3.4. Photocatalytic mechanisms

TRIANE. The positive holes (h^+) and the $OH^\bullet$ radicals, photogenerated by reaction of H_2O with positive holes (h^+) at the TiO_2 interface are the main active species in photocatalysis. Taking into account the electrophilic character of these species, the attack of TRIANE should occur on N^1 or N^2 atoms, which have the most important radical frontier density (see Table 2).

Table 2
Calculated radical frontier density for TRIANE, OH-TRIANE, Ph-TRIANE and Ph-TRIOLE using the MOPAC method from the CAChe system

	TRIANE	OH-TRIANE	Ph-TRIANE	Ph-TRIOLE
N^1	0.498	0.436	0.061	0.277
N^2	0.498	0.437	0.060	0.277
C^3	0.232	0.207	0.128	0.134
N^4	0.084	0.215	0.241	0.200
C^5	0.232	0.213	0.129	0.134
O^6	0.152	0.135	0.072	0.122
O^7	0.152	0.133	0.073	0.122
O^8		0.143		
C^8			0.306	0.178
C^9			0.187	0.115
C^{10}			0.125	0.066
C^{11}			0.283	0.195
C^{12}			0.122	0.066
C^{13}			0.193	0.114

The step (a) mentioned in Scheme 1 can be explained by the attack of $OH^\bullet$ radical on these nitrogen atoms to form a nitroso compound as tentatively mentioned below:

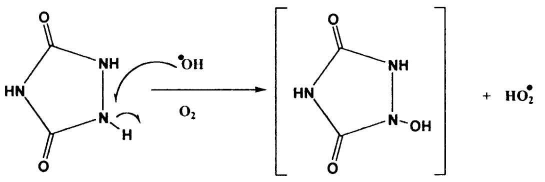

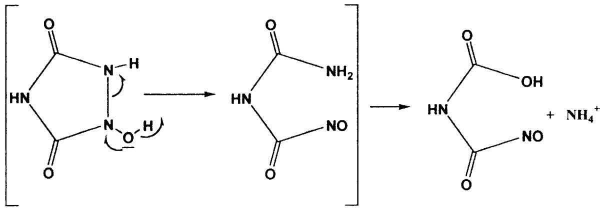

Amide structure has not been detected, however, it is known that it can be hydrolyzed into ammonium and acid. However, step (a) does not seem to be the major step of TRIANE photodegradation. Actually, first the amount of NH_4^+ formed from the beginning of degradation is small compared to the amount of N_2 gas initially detected (see Fig. 6(a)) and secondly the evolution of NO_3^- ions, which could come from nitroso intermediate compounds, 118 *m/z* or 74 *m/z*, detected, respectively, after 1 and 2 h of irradiation, should appear before 3 h of irradiation, that is not the case. The important detection of N_2 gas from the beginning of irradiation could be explained by the reactions of OH$^\bullet$ radicals or h$^+$ species on carbon atom of carbonyl group (b), as tentatively suggested below:

carbon atom attack of TRIANE by •OH radical:

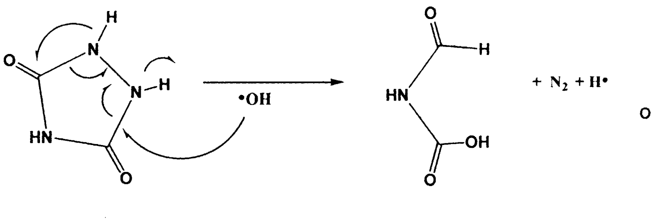

carbon atom attack of TRIANE by h$^+$ species

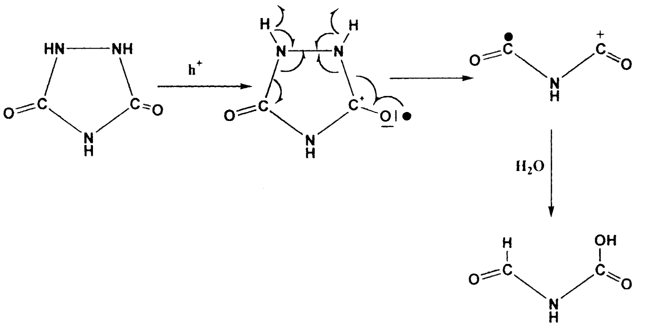

Carbon atom has a radical frontier density smaller than N^1 or N^2 atoms. However, the attack on this atom seems to be the major step. This phenomenon could be explained by the closeness of carbonyl group to the TiO_2 surface, induced by the adsorption. The nil slope of CO_2 evolution from the beginning of the degradation (see Fig. 5(a)) and the evolution of NH_4^+ ions from 2 h of irradiation (see Fig. 6(a)), time when NH_2–COOH was detected, confirm that step (b) is the major reaction, showing that the adsorption plays an important role as previously mentioned by one of us [22]. The two steps agree with the evolution of UV spectrum during irradiation time which indicate that in the first time a breaking of O=C–NH–NH–C=O occurred while O=C–NH–C=O structure persisted a longer time.

OH-TRIANE. The highest radical frontier density of N^1 and N^2 atom led to the attack of OH$^\bullet$ radical on these atoms (step (a) in Scheme 2). The photodegradation pathway is similar to those proposed for step (a) in the TRIANE degradation.

However, the attack by OH$^\bullet$ radical or by h$^+$ species on carbon atom of carbonyl group (step (b) in Scheme 2) is also suggested taking into account the significant amount of N_2 gas formed from the beginning of the degradation. In Scheme 3, a detail mechanism is suggested for the step (b) by using h$^+$ species, however, similar reaction can be also explained by using OH$^\bullet$ radical. As previously mentioned, step (b) could be favored by the adsorption of carbonyl group on TiO_2 surface. By similitude to the degradation of TRIANE, this step should led to the formation of OHC (or COOH)–N(OH)–COOH structure, which is not detected in solution. The absence of its detection could be due to its strong adsorption on TiO_2 by CO and OH groups which will favor the oxidation and decarboxylation by active species (OH$^\bullet$ and h$^+$) present at the TiO_2 surface. This hypothesis agrees with the important evolution of CO_2 from the beginning of the OH-TRIANE degradation (see Fig. 5(a)). In this case, HOHN–COOH will be quickly formed. The adsorption of OH-TRIANE by both the groups, OH and C=O, could also favor the breaking of RHON–COR_1 bond as tentatively suggested in Scheme 3 (reaction (1)).

RCO$^\bullet$ radical can either abstract an H of OH-TRIANE to form ON–CO–NH–NH–COH, which by reaction with OH$^\bullet$ radical is transformed into HOOC–HN–NH–CHO (reaction (3)) and H_2N–NH–CHO, ON–COOH (reaction (4)), respectively, or react on another OH-TRIANE molecule by attack of N^1 (or N^2) atom which has the highest electron density to form the 1,2,4,5-tetrazixane-3,6-dione, confirmed by LC/MS in positive mode (Scheme 3). The formation of this compound can explain the increase of UV spectrum after 2 h of irradiation. The simulation of the UV spectrum of 1,2,4,5-tetrazixane-3,6-dione agreed with the UV spectrum observed after 2 h and more in the degradation of OH-TRIANE. The formation of this compound is also observed in the degradation of TRIANE but at a longer irradiation time. The comparison of the degradation pathways of TRIANE and OH-TRIANE pointed out that adsorption and electron density were two important parameters in the photocatalytic reaction.

Ph-TRIANE. Based on all the above data and the species identified, a tentative degradation pathway is suggested in Scheme 4.

Taking into account the electrophilic character of OH$^\bullet$ radical, the attack of Ph-TRIANE should occur on C^8 or C^{11} atoms, which have the most important radical frontier density (Table 2). However, the attack on C^6 atom can be negligible due to the steric hindrance. The formation of a compound at 167 *m/z*, step (a), is consistent with the attack of OH$^\bullet$ on C^{11} atom. However, (i) the compound at 167 *m/z* also presents an opening of a heterocycle; (ii) a similar compound without OH on aromatic ring is also detected at the same irradiation time (compound at 151 *m/z*). The presence of this latter compound and the evolution of one CO_2 molecule (see Fig. 5) from the beginning of the degradation suggests that one of the initial Ph-TRIANE degradation corresponded to the attack by OH$^\bullet$ radical or by h$^+$ species on carbon atom of carbonyl group and then decarboxylation (step (b)). This step is similar to step (b) of TRIANE and OH-TRIANE degradation. However, in this case, either *N,N*-dicarboxylic aniline or 1-carboxy-4-phenyl semicarbazide are detected, probably because the formation of nitrogen radical is stabilized by aromatic ring as suggested below:

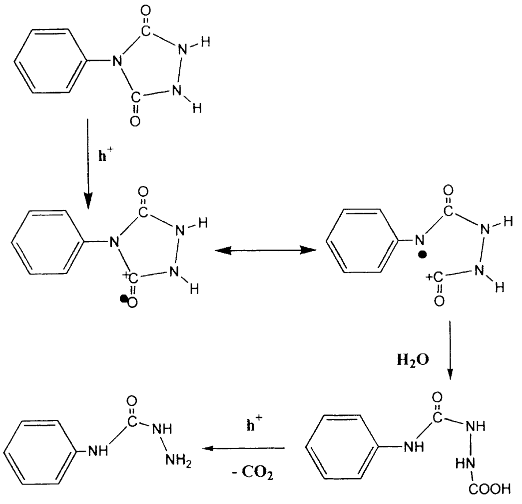

As previously suggested, the adsorption of Ph-TRIANE by CO group could be at the origin of this step (b). Indeed, due to the adsorption, C atom of CO group is closed to TiO_2 surface where active species are formed. The evolution of UV spectrum during the irradiation, i.e. increase of 239 nm UV band, and the simulation of UV spectrum of C_6H_5–NH–CO–N_2H_3 showing a UV band at this wavelength, suggested that the heterocycle opening is the most important initial step in the degradation of Ph-TRIANE. The evolution of N_2 gas from the beginning of irradiation and the absence of C_6H_5–NH–$(COOH)_2$ points out that the evolution of N_2 gas comes from the degradation of two initial compounds previously mentioned. The detection of an important peak of phenylformamide (M = 121 *m*/*z*) from 30 min agreed with this hypothesis. The absence of CO_2 evolution after 15 min of irradiation could be explained by the

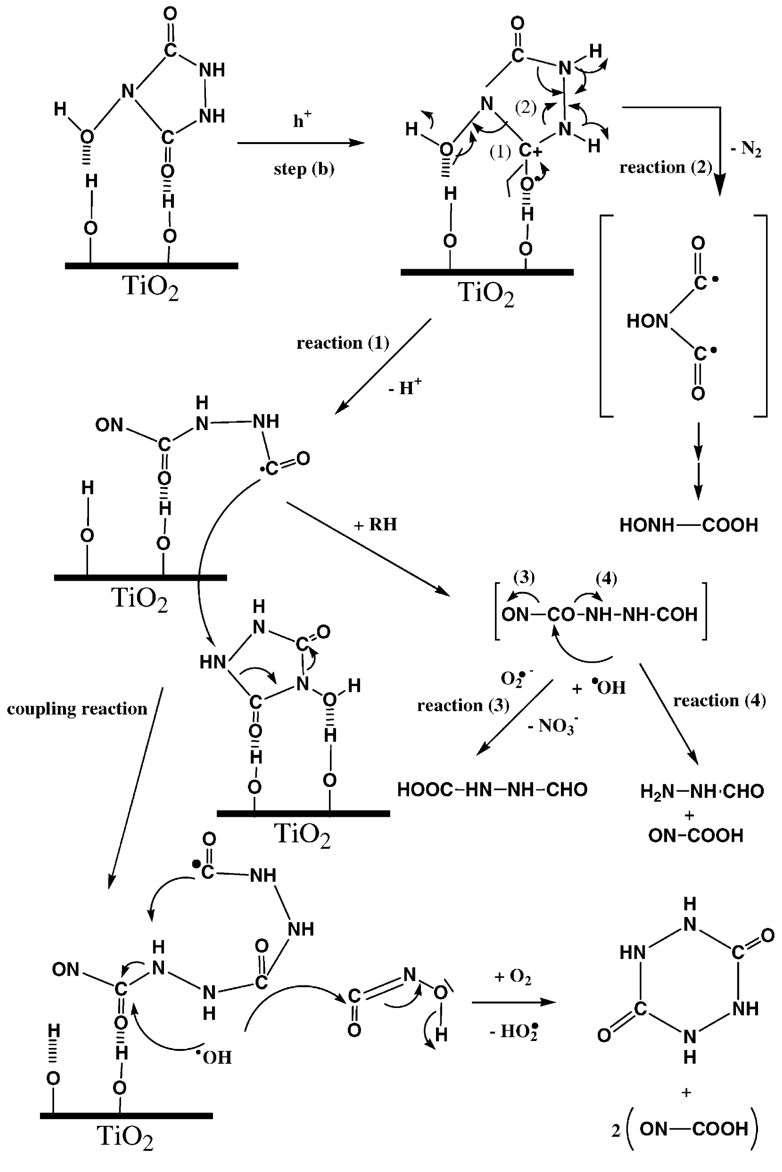

Scheme 3. Proposed pathway for the photodegradation of step (b) of OH-TRIANE.

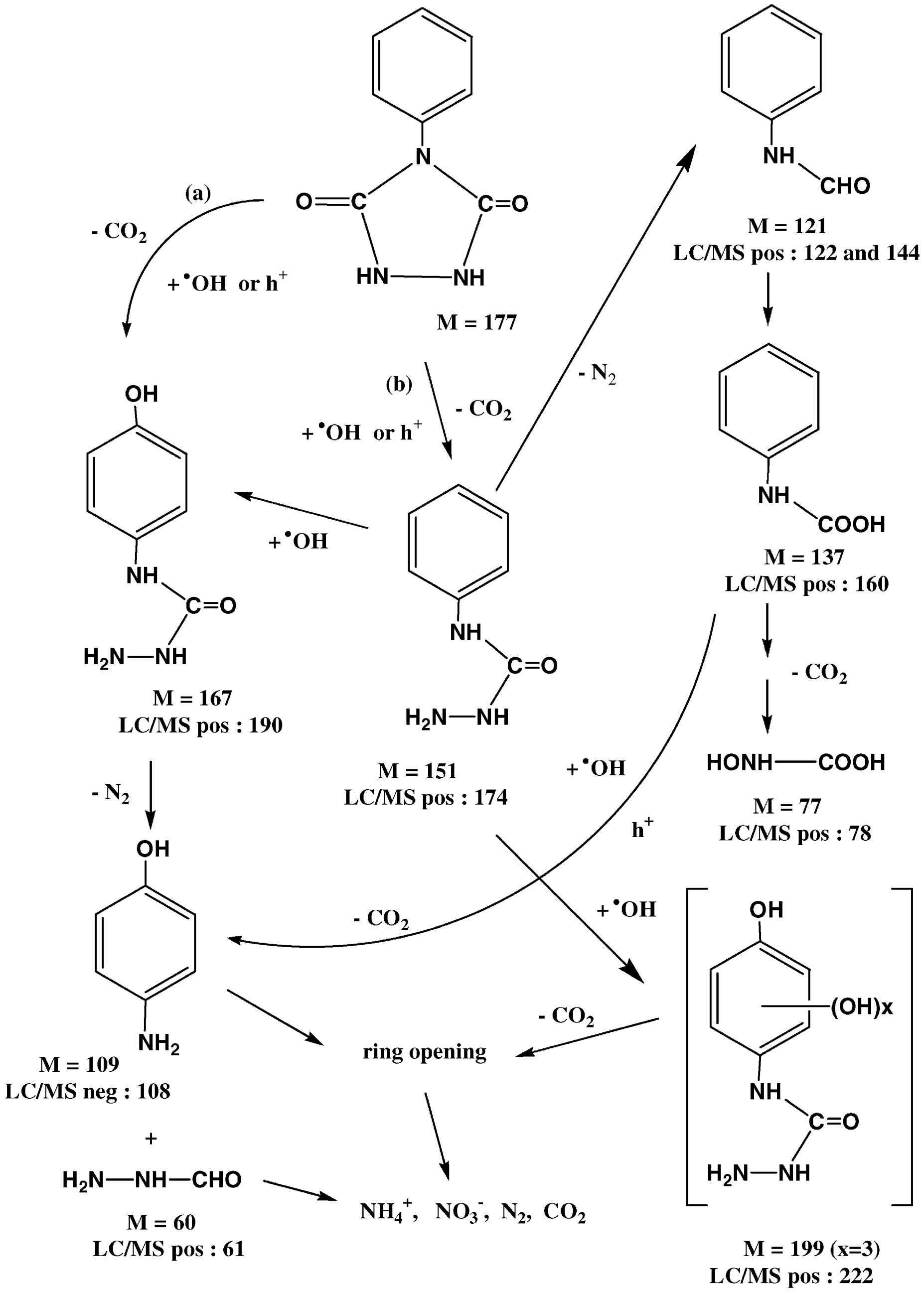

Scheme 4. Proposed pathway for the photodegradation of Ph-TRIANE.

hydroxylation of aromatic ring. Between 30 min and 7 h of irradiation, aldehyde group of phenylformamide was transformed into carboxylic group to form C_6H_5–NH–COOH and at the same time aromatic ring was little by little oxidized. For example, a compound having three hydroxyl groups on aromatic ring ($M = 199\,m/z$) was detected during this period. The important evolution of CO_2 after 8 h of irradiation was attributed to the opening of aromatic ring. The appearance of NH_2–NH–COH and its evolution after 11 h of irradiation showed that a part of aliphatic chain is slower than that for aromatic ring.

Ph-TRIOLE. The presence of a double bond in the heterocycle completely modified the degradation pathway (see Scheme 5). On the contrary to Ph-TRIANE, hydroxylation on N^1 and N^2 atoms occurred to form the compound at 209 *m/z* in Ph-TRIOLE (step (a)). The highest radical frontier density of N^1 and N^2 in Ph-TRIOLE and of C^8 in Ph-TRIANE, is at the origin of different behavior, showing the importance of radical frontier density. As previously noticed for the three other compounds, the attack on carbon atom of carbonyl is also observed (step (b)). However, in this case, dicarboxylic aniline is detected as already observed in

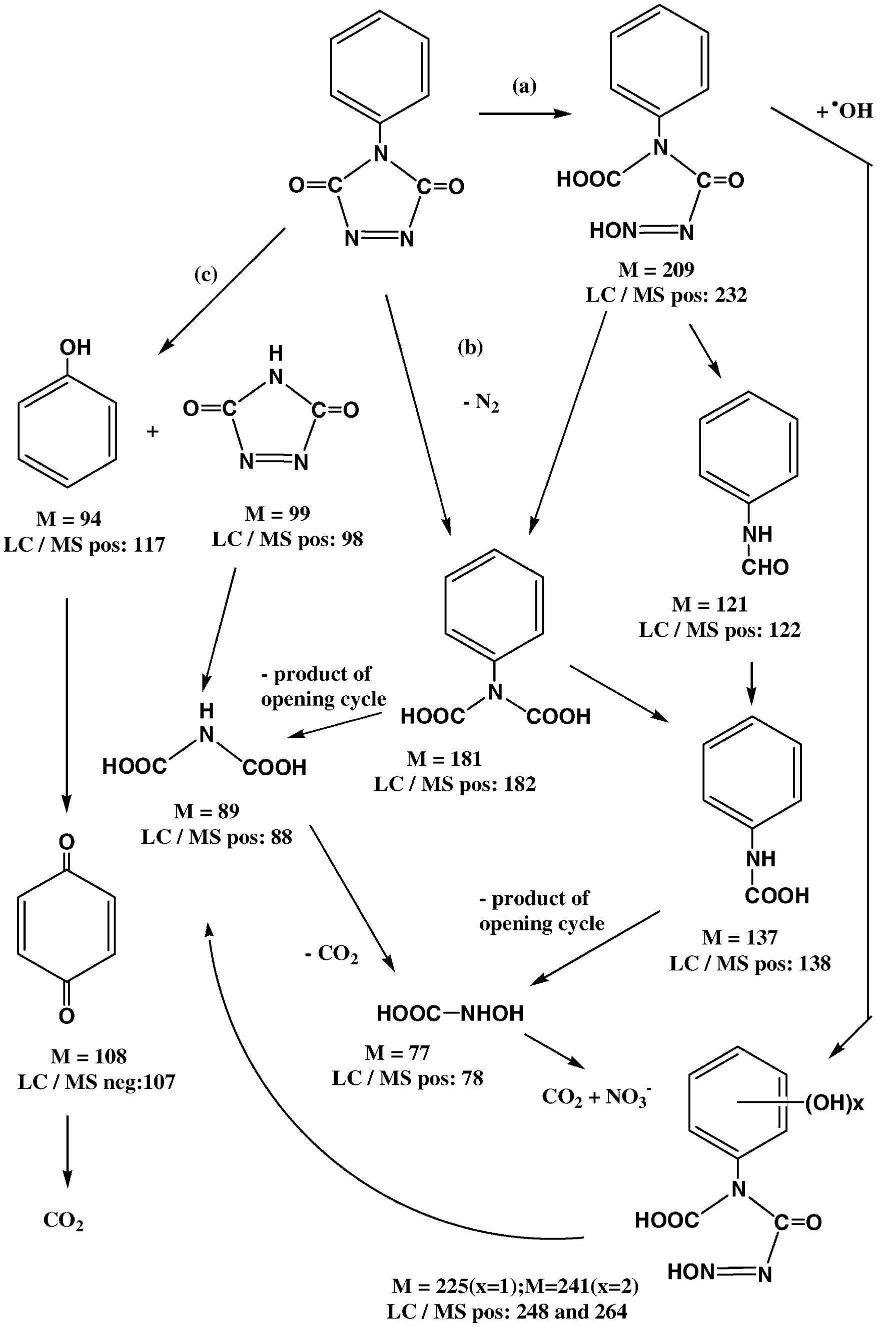

Scheme 5. Proposed pathway for the photodegradation of Ph-TRIOLE.

TRIANE while it is not present in Ph-TRIANE. The presence of a double bond between both the nitrogen atoms favors the removal of N_2 leading to dicarboxylic aniline. The third initial step corresponding to the breaking of C–N bond between aromatic ring and heterocycle was also observed. The relatively high radical frontier density of N^4 atom could explain the presence of this step. However, the same step should be occurring in the degradation of Ph-TRIANE but it is not observed.

4. Conclusions

This work showed the role of frontier orbital density and of adsorption on the degradation pathways. Two major pathways have been determined in the degradation of three triazolidine and one triazole structure, by using LC/MS, UV, gas chromatography and ion liquid chromatography. One corresponded to the attack of $OH^\bullet$ radical on the atom with the most important frontier electron densities as simulated by

MOPAC system. The second pathway was due to the attack on carbon atom of the carbonyl group. Considering that frontier electron densities was about 2.1–2.4 smaller than those found for the atom with the higher value, and that initial N_2 gas evolution was important, we inferred that adsorption, as predicted by computer simulation and confirmed by IR measurement, probably favored this pathway. We also suggested that h^+ species could be implicated in the mechanism. The study for the fate of nitrogen atom showed that two adjacent nitrogen atoms were mainly transformed into N_2 gas and to a lesser extent into $NH_4{}^+$ ions. For the four heterocycles studied, $NO_3{}^-$ was never detected at the beginning of the photodegradation even when OH substituent was present on the nitrogen atom of the CO–N–CO structure.

Acknowledgements

We are grateful to the Japanese Ministry of Education, Culture, Sports, Science and Technology (Grant-in-aid for Scientific Research No. 10640569 to HH) for generous support of our work.

References

[1] M. Schiavello (Ed.), Photocatalysis and Environment: Trends and Applications, Vol. 238, NATO ASI Series C, Kluwer Academic Publishers, Dordrecht, 1987.

[2] D.F. Ollis, H. Al-Ekabi (Eds.), Photocatalytic Purification and Treatment of Water and Air, Elsevier, Amsterdam, 1993.

[3] J.-M. Herrmann, C. Guillard, P. Pichat, Catal. Today 17 (1993) 7.

[4] P. Pichat, in: G. Ertl, H. Knözinger, J. Weitkamp (Eds.), Handbook of Heterogeneous Catalysis, Vol. 4, VCH, Weinheim, 1998, p. 2111 (Chapter 3.19).

[5] D. Bahnemann, J. Cunningham, M.A. Fox, E. Pelizzetti, P. Pichat, N. Serpone, in: G.R. Zepp, D.G. Crosby (Eds.), Aquatic and Surface Photochemistry, Lewis, Boca Raton, FL, 1994, p. 261.

[6] H. Hidaka, K. Nohara, J. Zhao, E. Pelizzetti, N. Serpone, J. Photochem. Photobiol. A 97 (1995) 145.

[7] S. Horikoshi, H. Hidaka, N. Serpone, J. Photochem. Photobiol. A 138 (2001) 69.

[8] M. Vautier, C. Guillard, J.M. Herrmann, J. Catal. 201 (2001) 4–6.

[9] D.M. Blake, Bibliography of work on the photocatalytic removal of hazardous compounds from water and air, NREL/TP-430-22197, National Renewable Energy Laboratory Golden Co., 1997 and 1999.

[10] M.A. Fox, M.T. Dulay, Chem. Rev. 93 (1993) 341.

[11] K.A. Gray, U. Stafford, Res. Chem. Intermed. 20 (8) (1994) 835.

[12] A. Mills, S. Le Hunte, J. Photochem. Photobiol. A 108 (1997) 1.

[13] L. Cerminati, P. Pichat, C. Guillard, A. Albini, J. Phys. Chem. B 101 (1997) 2650.

[14] P. Pichat, C. Guillard, L. Amalric, A.C. Renard, O. Plaidy, Sol. Energy Mater. Sol. Cells 38 (1995) 391.

[15] L. Amalric, C. Guillard, P. Pichat, Res. Chem. Intermed. 20 (1994) 579.

[16] S. Horikoshi, N. Serpone, S. Yoshizawa, J. Knowland, H. Hidaka, J. Photochem. Photobiol. A 120 (1999) 63.

[17] S.C. Guillard, J. Photochem. Photobiol. A 135 (2000) 65.

[18] P. Pichat, C. Guillard, C. Maillard, L. Amalric, J.C. D'Oliveira, in: D.F. Ollis, H. Al Elkabi (Eds.), Photocatalytic Purification and Treatment of Water and Air, Elsevier, Amsterdam, 1993, p. 207.

[19] L. Amalric, C. Guillard, E. Blanc-Brude, P. Pichat, Water Res. 30 (5) (1996) 1137.

[20] N. Jaffrezic-Renault, P. Pichat, A. Foissy, R. Mercier, J. Phys. Chem. 80 (1986) 2733.

[21] B. Smith, Infrared Spectral Interpretation: A Systematic Approach, CRC Press, Boca Raton, 1999, pages 133 and 247.

[22] G.K.C. Low, S.R. McEvoy, R.W. Mattews, Environ. Sci. Technol. 25 (1991) 460.

[23] A. Bravo, J. Garcia, X. Domenech, J. Peral, J. Chem. Res. 376 (1993).

[24] C. Maillard, These de Doctorat, Université Clauce Bernard Lyon I, February 19, 1993.